Stability Analysis and Bifurcation Control of Fractional-Order Double Memristor Hopfield Neural Networks with Time Delay *

Feng Liu[1,2,3], Luying Wang[1], Bo Zhang[1], Hua Wang[4], and Xiuqin Yang[5]

[1] School of Automation, China University of Geosciences, Wuhan, 430074, China*
fliu@cug.edu.cn
[2] Engineering Research Center of Ministry of education for intelligent technology of earth exploration
[3] Hubei key Laboratory of Advanced Control and Intelligent Automation for Complex Systems, Wuhan, 430074, China
[4] Department of Mechanical Engineering, Boston University, Boston, MA 02215, USA
[5] School of Education, Minzu University of China, Beijing, 100081, China

Abstract. In this paper, the stability and Hopf bifurcation of a class of fractional-order Hopfield neural networks with time delay and double memristors are discussed. The local stability of the equilibrium point of the system is discussed. Taking the time delay as the bifurcation parameter, the critical condition of Hopf bifurcation in the system is derived. In order to improve the stability of the system, by adding a state feedback controller to the network system, the stability of the system and the conditions for Hopf bifurcation are analyzed. The numerical simulation shows that the state feedback controller improves the dynamic performance of the system, the bifurcation point of the system is delayed, and the system obtains a larger parameter stability range.

Keywords: Fractional order Hopfield neural networks · memristor· stability · bifurcation control

1 Introduction

Human brain is the most complex nonlinear dynamic system known at present. In order to reveal the complex dynamic characteristics of the biological nervous system, researchers designed neural networks by imitating the behavior of biological neural networks to realize the reception [1], storage [2] and transmission of information [3]. In 1982, Hopfield proposed the famous Hopfield neural network model based on energy function [4], which has been widely used in associative memory, image processing, secure communication and other fields. From the perspective of dynamics, Hopfield neural network has rich dynamic characteristics, which has an important impact on the design and application of the

* Supported by National Natural Science Foundation (NSFC) of China under Grant 72274233, 61472374.

network. Due to the existence of special nonlinear neuron activation function in Hopfield Neural Network (HNN), it is an important tool to simulate the complex behavior of human brain [5].

Fractional calculus can describe physical phenomena more accurately [6]. As a kind of nonlinear resistance element with memory function, memristor becomes a natural non-volatile memory. Due to its high cost and technical complexity, much of the research relies on models and simulations. Different types of memristor models (such as cubic smooth [7] , quadratic smooth [8] , primary smooth [9] , and hyperbolic tangent [10] memristor models) have different nonlinear dynamic behaviors, and their introduction into neural network systems leads to richer dynamic characteristics, such as chaos and bifurcation phenomena.

Time delay is universal in neural networks. However, the introduction of time delay often causes changes in system stability, such as bifurcation [11], periodic oscillation [12], chaos [13] and so on. For example, the reference [14] studies the synchronization control of memristor complex valued neural networks with time delay. The synchronization problem of coupled neural networks with distributed delays is studied in the reference [15].

The memristor neural networks exhibit rich dynamic behaviors, mainly in stability, chaos and bifurcation. The global asymptotic stability of recurrent neural networks with discrete time-varying delays and distributed time-varying delays is studied in [16]. The highly correlated chaotic behavior of recurrent neural networks under structural connectivity in [17]. Reference [18] studies the integer bifurcation and chaotic behavior in memristor Chen system. Reference [19] discusses the zero-Hopf bifurcation behavior of memristor BAM neural network model with delay and diffusion. In the study of bifurcation and its control, researchers usually prevent, delay, or guide bifurcation phenomena by adjusting system parameters or introducing external controls. For example, literature [20] analyzed the dynamic behavior and control problem of Lesley-Gower predator-prey system, and literatur [21] discussed the Hopf bifurcation problem of the economic model, and proposed a time-delay feedback control scheme to control the bifurcation.

From the above narrative, we find that fractional-order memristor delay Hopfield neural network not only combines the advantages of fractional-order calculus and memristor, but also introduces the disturbance effect of time delay, which can simulate the complex behavior of neurons and its memory effect more accurately. In this paper, we construct a fractional order double memristor delay Hopfield neural network system, analyze the effects of time delay on the system, and simulate the effects of time delay on organisms in biological nervous systems.

2 Model description

The bidirectional electromagnetically induced current between neuron 1 and neuron 2 is simulated by a magnetic-controlled memristor. Its mathematical

model can be described as the following form

$$\begin{cases} i_M = G(y_1)\nu_M = k_1 y_1 \nu_M, \\ \dot{y}_1 = \nu_M, \end{cases} \tag{1}$$

where k_1 represents the coupling strength of neurons under electromagnetic induction, y_1 represents the magnetic flux of the memristor. $G(y_1) = k_1 y_1$ represents the derivative function, v_M and i_M represent the membrane potential difference between neuron 1 and neuron 2 and the induced current through the memristor, respectively.

The self-connecting synapse of neuron 2 is simulated by a quadratic nonlinear magneto-controlled memristor.Its mathematical model can be described as

$$\begin{cases} i = k_2(c - dy_2^2)\nu, \\ \dot{y}_2 = \nu - y_2, \end{cases} \tag{2}$$

where k_2 represents the coupling strength of the memristor synapse,y_2 represents the magnetic flux of the memristor,$G(y_2) = c - dy_2^2$ represents a derivative function,v and i Represents the membrane potential of neuron 2 and the current flowing through the memristor, respectively.

Based on the above two memristors, a fractional double memristor Hopfield neural network model is constructed, which is affected by electromagnetic induction and time delay. The system is as follows:

$$\begin{cases} D^\theta x_1(t) = -c_1 x_1(t) + a_{11}\tanh\left(x_1(t)\right) + a_{12}\tanh\left(x_2(t-\tau)\right) \\ \qquad\qquad +k_1 y_1(x_2(t) - x_1(t)), \\ D^\theta x_2(t) = -c_2 x_2(t) + a_{21}\tanh\left(x_1(t-\tau)\right) + k_2(c - dy_2^2)\tanh\left(x_2(t)\right) \\ \qquad\qquad -k_1 y_1(x_2(t) - x_1(t)), \\ D^\theta y_1 = x_2(t) - x_1(t), \\ D^\theta y_2 = \tanh\left(x_2(t)\right) - y_2, \end{cases} \tag{3}$$

where $\theta \in (0, 1]$ it's fractional, D^θ represents the fractional derivative of Caputo, $x_i(i = 1, 2)$ represents the membrane voltage of the i-th neuron,$y_i(i = 1, 2)$ represents the internal state variable of the memristor,Hyperbolic tangent function $\tanh(x_n)(n = 1, 2)$ represents the neuron activation function from the voltage input from the n-th neuron, and its coefficient a_{ij} is the mutual synaptic weight, indicating the connection strength,coefficient $c_i(i = 1, 2)$ it's a self-connecting synapse,τ are the time delay existing in the system.

3 Local stability and bifurcation analysis of uncontrolled systems

In this section, the delay is used as a bifurcation parameter to discuss the local stability of the equilibrium point of system (3) and the conditions of Hopf bifurcation. Then the linearized equation of the system at the origin O(0,0,0,0)

is as follows :

$$\begin{cases} D^{\theta}x_1(t) = -c_1x_1(t) + a_{11}x_1(t) + a_{12}x_2(t-\tau) + k_1y_1(x_2(t) - x_1(t)), \\ D^{\theta}x_2(t) = -c_2x_2(t) + a_{21}x_1(t-\tau) + k_2cx_2(t) - k_1y_1(x_2(t) - x_1(t)), \\ D^{\theta}y_1 = x_2(t) - x_1(t), \\ D^{\theta}y_2 = x_2(t) - y_2. \end{cases} \tag{4}$$

Applying the Laplace transform, the characteristic equation of system (4) is:

$$\begin{vmatrix} \lambda^{\theta} - J_{11} & -J_{12}^{'} - J_{12}^{''}e^{-\lambda\tau} & -J_{13} & 0 \\ -J_{21}^{'} - J_{21}^{''}e^{-\lambda\tau} & \lambda^{\theta} - J_{22} & -J_{23} & 0 \\ 1 & -1 & \lambda^{\theta} & 0 \\ 0 & -1 & 0 & \lambda^{\theta} + 1 \end{vmatrix} = 0. \tag{5}$$

where $J_{11} = -c_1 + a_{11} - k_1y_1, \quad J_{12}^{'} = k_1y_1, J_{12}^{''} = a_{12}, J_{13} = k_1(x_2 - x_1), J_{21}^{'} = k_1y_1, J_{21}^{''} = a_{21}, J_{22} = -c_2 + k_2c - k_1y_1, J_{23} = -k_1(x_2 - x_1)$.

The characteristic equation corresponding to equation (5) is as follows:

$$D(\lambda, \tau) = D_0(\lambda) + D_1(\lambda)e^{-\lambda\tau} + D_2(\lambda)e^{-2\lambda\tau} = 0, \tag{6}$$

where $D_0(\lambda) = \lambda^{4\theta} + b_1\lambda^{3\theta} + b_2\lambda^{2\theta} + b_3\lambda^{\theta} + b_4, D_1(\lambda) = b_5\lambda^{2\theta} + b_6\lambda^{\theta} + b_7$,
$D_2(\lambda) = b_8\lambda^{2\theta} + b_9\lambda^{\theta}, b_2 = -J_{11} - J_{22} - J_{13} + J_{23} + J_{22}J_{11} - J'_{21}J'_{12}$,
$b_3 = -J_{13} + J_{23} - J'_{21}J'_{12} - J_{23}J_{11} - J_{23}J'_{12} + J_{13}J'_{21} + J_{13}J_{22} + J_{11}J_{22}$,
$b_4 = -J_{11}J_{23} - J_{23}J_{12} + J_{13}J'_{21} + J_{13}J_{22}, b_5 = -J'_{12}J''_{21} - J''_{12}J'_{21}$,
$b_6 = -J'_{12}J''_{21} - J'_{21}J''_{12} - J''_{12}J_{23} + J''_{21}J_{13}, b_1 = 1 - J_{11} - J_{22}$,
$b_7 = -J''_{12}J_{23} + J''_{21}J_{13}, b_8 = J''_{21}J''_{12}, b_9 = -J''_{21}J''_{12}$.

According to the characteristic equation, the stability of the equilibrium point is divided into the following two cases.

Case 1. When $\tau = 0$, the system characteristic equation is

$$P = \lambda^{4\theta} + m_1\lambda^{3\theta} + m_2\lambda^{2\theta} + m_3\lambda^{\theta} + m_4 = 0 \tag{7}$$

where $m_1 = b_1, m_2 = b_2 + b_5 + b_8, m_3 = b_3 + b_6 + b_9, m_4 = b_4 + b_7$.

Lemma 1. *For the following fractional order system: $D^{\theta}x(t) = Ax(t), A \in R^{n\times n}$, the equilibrium point of the system is locally asymptotically stable if all eigenvalues $\lambda_i (i = 1, 2...n)$ satisfy $|\arg(\lambda_i)| > \frac{\theta\pi}{2}$, where $\theta \in (0, 1]$.*

Then according to Lemma 1 and Routh-Hurwitz stability criterion, we have:

Theorem 1. *The system (3) is locally asymptotically stable if and only if $\Delta_i > 0 (i = 1, 2, 3, 4)$ is true, where Δ_i is defined as follows:*

$$\Delta_1 = m_1, \Delta_2 = \begin{vmatrix} m_1 & m_3 \\ 1 & m_2 \end{vmatrix}, \Delta_3 = \begin{vmatrix} m_1 & m_3 & 0 \\ 1 & m_2 & m_4 \\ 0 & m_1 & m_3 \end{vmatrix}, \Delta_4 = m_4\Delta_3.$$

Case 2. When $\tau > 0$, to simplify this equation, we multiply both sides of the equation by $e^{\lambda\tau}$, in which case equation (6) is reduced to the following:

$$D_0(\lambda)e^{\lambda\tau} + D_1(\lambda) + D_2(\lambda)e^{-\lambda\tau} = 0. \tag{8}$$

Let $\lambda = iw = w(\cos\frac{\pi}{2} + i\sin\frac{\pi}{2})(w > 0)$ be the root of the system, then substitute this value into the characteristic equation, separating the real and imaginary parts, and get:

$$\begin{cases} U_2 + (U_1 - U_3)\cos\omega\tau - (\eta_1 + \eta_3)\sin\omega\tau = 0, \\ \eta_2 + (\eta_1 - \eta_3)\cos\omega\tau - (U_1 + U_3)\sin\omega\tau = 0, \end{cases} \tag{9}$$

where $U_1 = \omega^{4\theta}\cos 2\theta\pi + b_1\omega^{3\theta}\cos\frac{3\theta\pi}{2} + b_2\omega^{2\theta}\cos\theta\pi + b_3\omega^{\theta}\cos\frac{\theta\pi}{2} + b_4, \eta_1 = \omega^{4\theta}\sin 2\theta\pi + b_1\omega^{3\theta}\sin\frac{3\theta\pi}{2} + b_2\omega^{2\theta}\sin\theta\pi + b_3\omega^{\theta}\sin\frac{\theta\pi}{2}, U_2 = b_5\omega^{2\theta}\cos\theta\pi + b_6\omega^{\theta}\cos\frac{\theta\pi}{2} + b_7, \eta_2 = b_5\omega^{2\theta}\sin\theta\pi + b_6\omega^{\theta}\sin\frac{\theta\pi}{2}, U_3 = b_8\omega^{2\theta}\cos\theta\pi + b_9\omega^{\theta}\cos\frac{\theta\pi}{2}, \eta_3 = b_8\omega^{2\theta}\sin\theta\pi + b_9\omega^{\theta}\sin\frac{\theta\pi}{2}$.

According to formula (9), and it can be obtained that

$$\begin{cases} \cos\omega\tau = -\frac{U_2(U_1+U_3)+\eta_2(\eta_1+\eta_3)}{U_1^2-U_3^2+\eta_1^2-\eta_3^2}, \\ \sin\omega\tau = \frac{U_2(\eta_1+\eta_3)-\eta_2(U_1+U_3)}{U_1^2-U_3^2+\eta_1^2-\eta_3^2}. \end{cases} \tag{10}$$

From equation (10), it can be obtained:

$$\tau_i^{(k)} = \frac{1}{\omega_i}\left[\arccos\left(-\frac{U_2(U_1+U_3)+\eta_2(\eta_1+\eta_3)}{U_1^2-U_3^2+\eta_1^2-\eta_3^2}\right) + 2k\pi\right], k = 0, 1, 2, \ldots. \tag{11}$$

where we take

$$\tau_0 = \tau_{i0} = \min_{i=1,2,\ldots}\{\tau_i\}, \omega_0 = \omega_{i_0}. \tag{12}$$

Then at $\tau = \tau_0$, we have a pair of pure imaginary roots of the equation, and at $\tau \in [0, \tau_0)$, the roots of the equation have negative real parts. Let $\lambda(\tau) = u(\tau) + iw(\tau)(w > 0)$ be the root of equation (9) satisfying $\lim_{\tau\to\tau_0} u(\tau_i^k) = 0, \lim_{\tau\to\tau_0} w(\tau_i^k) = w_0$ near $\tau = \tau_i^{(k)}$. By taking the derivative of τ in the characteristic equation (9), the following formula can be obtained:

$$\frac{d\lambda}{d\tau} = \frac{\alpha_1(w_0,\tau_0) + \alpha_2(w_0,\tau_0)}{\beta_1(w_0,\tau_0) + \beta_2(w_0,\tau_0)}, \tag{13}$$

and

$$\mathrm{Re}[\frac{d\lambda}{d\tau}] = \frac{\alpha_1(w_0,\tau_0)\beta_1(w_0,\tau_0) + \alpha_2(w_0,\tau_0)\beta_2(w_0,\tau_0)}{\beta_1^2(w_0,\tau_0) + \beta_2^2(w_0,\tau_0)}. \tag{14}$$

Obviously $\beta_1^2(w_0,\tau_0) + \beta_2^2(w_0,\tau_0)$ must be greater than 0, so we can get:

$$sign\left\{Re\left[\frac{\mathrm{d}\lambda}{\mathrm{d}\tau}\right]|_{\tau=\tau_0}\right\} = sign\left\{\alpha_1(w_0,\tau_0)\beta_1(w_0,\tau_0) + \alpha_2(w_0,\tau_0)\beta_2(w_0,\tau_0)\right\}.$$

If condition (H1)$sign\{Re[\frac{\mathrm{d}\lambda}{\mathrm{d}\tau}]\} \neq 0$, then transversal condition $Re\left[\frac{\mathrm{d}\lambda}{\mathrm{d}\tau}\right]|_{\tau=\tau_0} \neq 0$ holds.

Based on the above analysis, the following theorems can be obtained :

Theorem 2. *For the system (3), assume (H1) is true.*

(1) If $\tau \in [0, \tau_0)$, the system is locally asymptotically stable at the equilibrium point O;

(2) If $\tau > \tau_0$, the system is unstable at the equilibrium point O, and a Hopf bifurcation occurs at O at $\tau = \tau_0$.

4 Stability and bifurcation analysis of controlled systems

In this section, a state feedback controller is added to the fractional-order delay dual memristor system to improve the dynamic performance of the system, increase the critical delay of Hopf bifurcation and delay the Hopf bifurcation point of the system. It is essential to enhance the robustness of the system so that it can remain stable in the face of stronger disturbances. The controller model in this section is represented as follows:

$$U(t) = \delta[x(t) - x(t-\tau)],$$

where δ represents the feedback gain and τ represents the delay inside the feedback controller.

We add the state feedback controller to the first item of the system, then the system model is as follows:

$$\begin{cases} D^\theta x_1(t) = -c_1 x_1(t) + a_{11}\tanh(x_1(t)) + a_{12}\tanh(x_2(t-\tau)) \\ \qquad\quad +k_1 y_1(x_2(t) - x_1(t)) + \delta(x_2(t) - x_2(t-\tau)), \\ D^\theta x_2(t) = -c_2 x_2(t) + a_{21}\tanh(x_1(t-\tau)) + k_2(c - dy_2^2)\tanh(x_2(t)) \\ \qquad\quad -k_1 y_1(x_2(t) - x_1(t)), \\ D^\theta y_1 = x_2(t) - x_1(t), \\ D^\theta y_2 = \tanh(x_2(t)) - y_2. \end{cases} \tag{15}$$

Obviously, we get the same balance point for uncontrolled and controlled systems. Then the linearized system at the origin O is as follows

$$\begin{cases} D^\theta x_1(t) = -c_1 x_1(t) + a_{11} x_1(t) + a_{12} x_2(t-\tau) + k_1 y_1(x_2(t) - x_1(t)) \\ \qquad\quad +\delta(x_2(t) - x_2(t-\tau)), \\ D^\theta x_2(t) = -c_2 x_2(t) + a_{21} x_1(t-\tau) + k_2 c x_2(t) - k_1 y_1(x_2(t) - x_1(t)), \\ D^\theta y_1 = x_2(t) - x_1(t), \\ D^\theta y_2 = x_2(t) - y_2. \end{cases} \tag{16}$$

Then the characteristic equation of the system is:

$$\begin{vmatrix} \lambda^\theta - T_{11} & -T_{12}^{'} - T_{12}^{''} e^{-\lambda\tau_1} & -T_{13} & 0 \\ -T_{21}^{'} - T_{21}^{''} e^{-\lambda\tau_2} & \lambda^\theta - T_{22} & -T_{23} & 0 \\ 1 & -1 & \lambda^\theta & 0 \\ 0 & -1 & 0 & \lambda^\theta + 1 \end{vmatrix} = 0. \tag{17}$$

where $T_{11} = -c_1 + a_{11} - k_1 y_1, \quad T_{12}^{'} = k_1 y_1 + \delta, T_{12}^{''} = a_{12} - \delta, T_{13} = k_1(x_2 - x_1), T_{21}^{'} = k_1 y_1, T_{21}^{''} = a_{21}, T_{22} = -c_2 + k_2 c - k_1 y_1, T_{23} = -k_1(x_2 - x_1)$.

The characteristic equation of system (15) is:

$$P(\lambda,\tau)=P_0(\lambda)+P_1(\lambda)e^{-\lambda\tau}+P_2(\lambda)e^{-2\lambda\tau}=0. \tag{18}$$

where $P_0(\lambda)=\lambda^{4\theta}+l_1\lambda^{3\theta}+l_2\lambda^{2\theta}+l_3\lambda^{\theta}+l_4, P_1(\lambda)=l_5\lambda^{2\theta}+l_6\lambda^{\theta}+l_7, P_2(\lambda)=l_8\lambda^{2\theta}+l_9\lambda^{\theta}, l_1=1-T_{11}-T_{22}, l_2=-T_{11}-T_{22}-T_{13}+T_{23}+T_{22}T_{11}-T_{21}^{'}T_{12}^{'}, l_3=-T_{13}+T_{23}-T_{21}^{'}T_{12}^{'}-T_{23}T_{11}-T_{23}T_{12}^{'}+T_{13}T_{21}^{'}+T_{13}T_{22}+T_{11}T_{22}, l_4=-T_{11}T_{23}-T_{23}T_{12}+T_{13}T_{21}^{'}+T_{13}T_{22}, l_5=-T_{12}^{'}T_{21}^{''}-T_{12}^{''}T_{21}^{'}, l_6=-T_{12}^{'}T_{21}^{''}-T_{21}^{'}T_{12}^{''}-T_{12}^{''}T_{23}+T_{21}^{''}T_{13}, l_7=-T_{12}^{''}T_{23}+T_{21}^{''}T_{13}, l_8=T_{21}^{''}T_{12}^{''}, l_9=-T_{21}^{''}T_{12}^{''}$.

To simplify this equation, we multiply both sides of the equation by $e^{\lambda\tau}$, in which case equation (18) is reduced to the following:

$$P_0(\lambda)e^{\lambda\tau}+P_1(\lambda)+P_2(\lambda)e^{-\lambda\tau}=0. \tag{19}$$

At this time, we only study the effect When $\tau>0$, let $\lambda=iw=w(\cos\frac{\pi}{2}+i\sin\frac{\pi}{2})(w>0)$, put it into the characteristic equation, separate the real and imaginary parts can be obtained:

$$\begin{cases} M_2+(M_1-M_3)\cos\omega\tau-(N_1+N_3)\sin\omega\tau=0,\\ N_2+(N_1-N_3)\cos\omega\tau-(M_1+M_3)\sin\omega\tau=0, \end{cases} \tag{20}$$

where $M_1=\omega^{4\theta}\cos 2\theta\pi+b_1\omega^{3\theta}\cos\frac{3\theta\pi}{2}+b_2\omega^{2\theta}\cos\theta\pi+b_3\omega^{\theta}\cos\frac{\theta\pi}{2}+b_4, N_1=\omega^{4\theta}\sin 2\theta\pi+b_1\omega^{3\theta}\sin\frac{3\theta\pi}{2}+b_2\omega^{2\theta}\sin\theta\pi+b_3\omega^{\theta}\sin\frac{\theta\pi}{2}, M_2=b_5\omega^{2\theta}\cos\theta\pi+b_6\omega^{\theta}\cos\frac{\theta\pi}{2}+b_7, N_2=b_5\omega^{2\theta}\sin\theta\pi+b_6\omega^{\theta}\sin\frac{\theta\pi}{2}, M_3=b_8\omega^{2\theta}\cos\theta\pi+b_9\omega^{\theta}\cos\frac{\theta\pi}{2}, N_3=b_8\omega^{2\theta}\sin\theta\pi+b_9\omega^{\theta}\sin\frac{\theta\pi}{2}$.

By simplifying equation (20), we can get:

$$\begin{cases} \cos\omega\tau=-\frac{M_2(M_1+M_3)+N_2(N_1+N_3)}{M_1^2-M_3^2+N_1^2-N_3^2},\\ \sin\omega\tau=\frac{M_2(N_1+N_3)-N_2(M_1+M_3)}{M_1^2-M_3^2+N_1^2-N_3^2}. \end{cases} \tag{21}$$

According to the previous analysis of uncontrolled systems, we also derive the conditions for Hopf bifurcation in controlled systems.

Lemma 2. *If w_1 makes $H(w)=0$, then when $\tau=\tau_1$, the eigenequation has a pair of pure imaginary roots $\pm w_1$, where*

$$\tau_i^j=\frac{1}{w_i}(arc\cos(-\frac{M_2(M_1+M_3)+N_2(N_1+N_3)}{M_1^2-M_3^2+N_1^2-N_3^2}+2k\pi), j=0,1,2,...,$$

$$\tau_1=\tau_{i1}=\min_{i=1,2,...}\{\tau_i\}, \omega_1=\omega_{i_1}.$$

Lemma 3. *Let $\lambda(\tau)=\varsigma(\tau)+iw(\tau)(w>0)$ be the root of equation(21)satisfying $\lim_{\tau\to\tau_1}\varsigma(\tau_i^j)=0, \lim_{\tau\to\tau_1}w(\tau_i^j)=w_1$ near τ_i^j. So the condition for Hopf bifurcation is $\mathrm{Re}[\frac{d\lambda}{d\tau}]|_{w=w_1,\tau=\tau_1}\neq 0$.*

Proof. By differentiating τ in the characteristic equation (18), the following formula can be obtained:

$$\frac{d\lambda}{d\tau} = \frac{A_1(w_1,\tau_1) + A_2(w_1,\tau_1)}{B_1(w_1,\tau_1) + B_2(w_1,\tau_1)},$$

and

$$\mathrm{Re}[\frac{d\lambda}{d\tau}] = \frac{A_1(w_1,\tau_1)B_1(w_1,\tau_1) + A_2(w_1,\tau_1)B_2(w_1,\tau_1)}{B_1^2(w_1,\tau_1) + B_2^2(w_1,\tau_1)}.$$

Then,

$$sign\left\{Re\left[\frac{\mathrm{d}\lambda}{\mathrm{d}\tau}\right]|_{\tau=\tau_1}\right\} = sign\left\{A_1(w_1,\tau_1)B_1(w_1,\tau_1) + A_2(w_1,\tau_1)B_2(w_1,\tau_1)\right\}.$$

Then, when condition (H2) $sign\left\{Re\left[\frac{\mathrm{d}\lambda}{\mathrm{d}\tau}\right]|_{\tau=\tau_1}\right\} \neq 0$ holds, the system satisfies Hopf bifurcation condition.

Based on the above analysis, the following theorem can be obtained:

Theorem 3. *If condition (H2) is true.*

(1) When $\tau \in [0, \tau_1)$, the system is locally asymptotically stable at the equilibrium point O;

(2) When $\tau > \tau_1$, the system is unstable at the equilibrium point O, and at $\tau = \tau_1$, a Hopf bifurcation occurs at O.

5 Numerical simulation

For the uncontrolled system (3) and the controlled system (15), we set the corresponding system parameters to verify the correctness of the theoretical analysis, and study the influence of time-delay τ on the system.

For uncontrolled systems (3) set the parameter to $c_1 = c_2 = k_2 = c = 1, a_{11} = -0.1, a_{12} = 4, a_{21} = -3.4, k_1 = 0.17, d = 0.4$. Let the initial value be (0.1,0.1,0.1,0.1) and the fractional order θ be 0.95. Then the system is:

$$\begin{cases} D^\theta x_1(t) = -x_1(t) - 0.1\tanh(x_1(t)) + 4\tanh(x_2(t-\tau)) + 0.17y_1(x_2(t) - x_1(t)), \\ D^\theta x_2(t) = -x_2(t) - 3.4\tanh(x_1(t-\tau)) + (1 - 0.4y_2^2)\tanh(x_2(t)) \\ \qquad\qquad -0.17y_1(x_2(t) - x_1(t)), \\ D^\theta y_1 = x_1(t) - y_1, \\ D^\theta y_2 = \tanh(x_2(t)) - y_2. \end{cases}$$

At this time, according to the above parameters and equations, we can simulate and analyze the fractional-order memristor neural networks :

(1) According to equation (11), we can get the critical delay point τ_0 =0.06. Obviously, we can see that τ_0 is small, which means that the system can only be stable with a small delay, and the system bifurcates into chaos by period-doubling at $\tau = 0.47$. Secondly, the stability of the system is analyzed according to the sequence diagram and phase diagram of the system. First, in $\tau = 0$, we

can calculate $\Delta_i > 0$, verifying the validity of Lemma 1 and theorem 1, that the equilibrium point of the system is locally asymptotically stable under the condition of no delay (as shown in Figure 1). When the value is $\tau = 0.05 < \tau_0$, the system is in a stable state (as shown in Figure 2). As can be seen from the figure, with the increase of time, the neuronal variables eventually tend to a stable state, and the generated periodic solutions are evenly distributed in space. When $\tau = 0.07 > \tau_0$, the system is in an unstable state (see Figure 3). As can be seen from the figure, the neuronal variables do not tend to be stable with the increase of time, and the generated periodic solutions are not uniform in space, at which time the system generates multiple limit cycles.

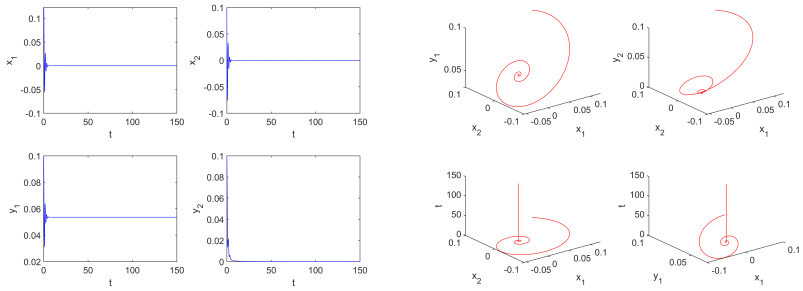

Fig. 1. When $\theta = 0.95, \tau = 0$, the waveform graph and phase diagram of system (3), the equilibrium point is locally asymptotically stable.

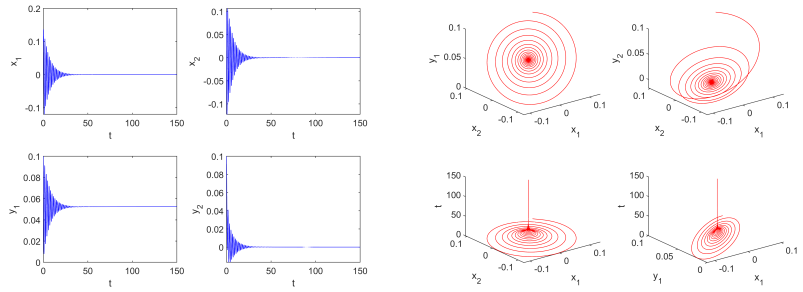

Fig. 2. When $\theta = 0.95, \tau = 0.05 < \tau_0$, the waveform graph and phase diagram of system (3), the equilibrium point is locally asymptotically stable.

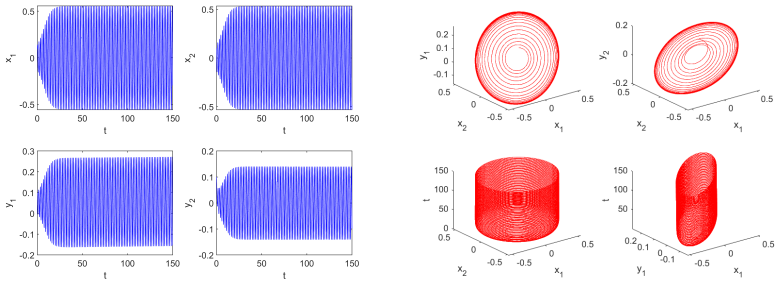

Fig. 3. When $\theta = 0.95, \tau = 0.07 > \tau_0$, the waveform graph and phase diagram of system (3), the equilibrium point is unstable and the system Hopf bifurcation occurs.

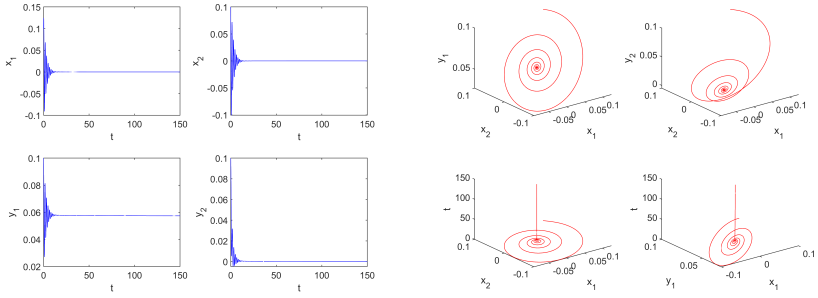

Fig. 4. When $\theta = 0.95, \tau = 0.07 < \tau_1$, the waveform graph and phase diagram of system (15), the equilibrium point is stable.

(2) Set parameter $\delta = 4$ for the controlled system, and the other parameters are the same as those for the uncontrolled system.

$$\begin{cases} D^\theta x_1(t) = -x_1(t) - 0.1\tanh(x_1(t)) + 4\tanh(x_2(t-\tau)) + 0.17y_1(x_2(t) - x_1(t)) \\ \qquad\qquad +4(x_2(t) - x_2(t-\tau)), \\ D^\theta x_2(t) = -x_2(t) - 3.4\tanh(x_1(t-\tau)) + (1 - 0.4y_2^2)\tanh(x_2(t)) \\ \qquad\qquad -0.17y_1(x_2(t) - x_1(t)), \\ D^\theta y_1 = x_1(t) - y_1, \\ D^\theta y_2 = \tanh(x_2(t)) - y_2. \end{cases}$$

By calculating and comparing with the bifurcation diagram (5), we get the critical delay $\tau_1 = 0.115$. Compared to an uncontrolled system, the critical delay increases and the bifurcation point delays, which means that the system can remain stable over a wider range of delays. When $\tau = 0.07 < \tau_1$, in the uncontrolled system, the system cannot reach stability, resulting in Hopf branching, while in the controlled system, the system is in a stable state under the action of the controller (as shown in Figure 4), thus verifying the role of the controller on the system.

6 Conclusion

In this paper, the stability and bifurcation characteristics of a class of fractional-order double memristive Hopfield neural networks with time delay are studied,Two memristors are selected, one is used to characterize the electromagnetic induction effect of the system, and the other is used to simulate the coupling between memristor synapses. The local stability of the equilibrium point of the system is analyzed, the time delay is selected as the bifurcation parameter, the bifurcation behavior of the system is analyzed. Then, a state feedback controller is designed to control the bifurcation of the system, so that the system can maintain stability and increase the robustness of the system. The numerical simulation shows that the system with the controller expands the stability range of the original system and achieves the ideal control effect.

The authors will continue to study memristor based neural networks in depth, especially in the following two aspects of future work: first, the study of more complex systems. The memristor is used as a connection synapse to form a complex neural network model by coupling multiple neurons. Compared with traditional neural networks, the coupled model is more complex and variable. Second, explore more complex dynamic behaviors and applications. In addition to stability and bifurcation phenomena, deeper dynamical properties such as hyperchaos and attractors will also be looked at, which are of great importance for practical applications such as encrypted communications.

References

1. Rebentrost P, Bromley T R, Weedbrook C, et al. Quantum Hopfield neural network[J]. Physical Review A,2018,98(4):042308.
2. Wang Z, Joshi S, Savel'Ev S, et al. Fully memristive neural networks for pattern classification with unsupervised learning[J]. Nature Electronics, 2018, 1(2): 137-145.
3. Danca M-F,Kuznetsov N V. Hidden chaotic sets in a Hopfield neural system [J], Chaos Solitons And Fractals, 2017, 103: 144-150.
4. Hopfield J J. Neurons with graded response have collective computational properties like those of two-state neurons. Proceedings of The National Academy of Sciences, 1984,81(10):3088-3092.
5. Bao B, Qian H, Xu Q, et,al. Coexisting behaviors of asymmetric attractors in hyperbolic-type memristor based Hopfield neural network[J].Frontiers in Computational Neuroscience, 2017,11:81-81.
6. Batiha I M, Albadarneh R B, Momani S, et al. Dynamics analysis of fractional-order Hopfield neural networks[J]. International Journal of Biomathematics, 2020, 13(08): 2050083.
7. Muthuswamy B. Implementing memristor based chaotic circuits[J].In ternational Journal of Bifurcation and Chaos, 2010, 20(05): 1335-1350.
8. Wang C, Zhou L, Wu R. The design and realization of a hyper-ch aotic circuit based on a flux-controlled m emristor with linear m em ductance[J]. Journal of Circuits, Systems and Computers, 2018, 27(03): 1850038.
9. Bao B C, Hu A H, Bao H, et al. Three-dimensional memristive Hindmarsh-Rose neuron model with hidden coexisting asymmetric behaviors[J]. Complexity, 2018, 2018: 3872573.

10. Bao B,Qian H,XU Q, et al. Coexisting behaviors of asymmetric attractors in hyperbolic-type memristor based Hopfield neural network[J].Frontiers in Computational Neuroscience11, 2017, 11:81.
11. Wan Q, Li F, Chen S, et al. Symmetric multi-scroll attractors in magnetized Hopfield neural network under pulse controlled memristor and pulse current stimulation[J]. Chaos, Solitons and Fractals, 2023, 169: 113259.
12. Ma Y, Lin Y, Dai Y. Stability and Hopf Bifurcation Analysis of A Fractional-Order BAM Neural Network with Two Delays Under Hybrid Control[J]. Neural Processing Letters, 2024, 56(2): 1-26.
13. Wan Q, Yan Z, Li F, et al. Complex dynamics in a Hopfield neural network under electromagnetic induction and electromagnetic radiation[J]. Chaos: An Interdisciplinary Journal of Nonlinear Science, 2022, 32(7): 073107
14. Zhu S, Liu D, Yang C, et al. Synchronization of memristive complex-valued neural networks with time delays via pinning control method[J]. IEEE Transactions on Cybernetics, 2019, 50(8): 3806-3815.
15. He W, Qian F, Cao J. Pinning-controlled synchronization of delayed neural networks with distributed-delay coupling via impulsive control[J]. Neural Networks, 2017, 85: 1-9.
16. Zeng H.He Y, Shi P, et al. Dissipativity analysis of neural networks with time-varyingdelays[J]. Neurocomputing, 2015,168:741-746.
17. Landau I D, Sompolinsky H. Coherent chaos in a recurrent neural network with structured connectivity[J]. PLoS computational biology, 2018, 14(12): e1006309.
18. Jiang X, Li J, Li B, et. al., Bifurcation, chaos, and circuit realization of a new four-dimensional memristor system, International Journal of Nonlinear Sciences and Numerical Simulation, 2022, 24(7): 2639-2648.
19. Zhou W, Fu B, Wang G. Time-Delay Memristive Recurrent Neural Network and Its Complex Dynamics[J]. International Journal of Bifurcation and Chaos, 2022, 32(10): 2250150.
20. Jiang X, Chen X, et al. Bifurcation and control for a predator-prey system with two delays, IEEE Transactions on Circuits and Systems-II: Express Brief, 2021, 68(1): 376-380.
21. Jiang X, Chen X, et al. On Hopf bifurcation and control for a delay systems, Applied Mathematics and Computation, 2020, 370: 124906.